AIP Applied Physics Letters

Exchange-biased magnetic tunnel junctions with antiferromagnetic -Mn3Ga

H. Kurt, K. Rode, H. Tokuc, P. Stamenov, M. Venkatesan, and J. M. D. Coey

Citation: Applied Physics Letters **101**, 232402 (2012); doi: 10.1063/1.4768941
View online: http://dx.doi.org/10.1063/1.4768941
View Table of Contents: http://scitation.aip.org/content/aip/journal/apl/101/23?ver=pdfcov
Published by the AIP Publishing

Exchange-biased magnetic tunnel junctions with antiferromagnetic ε-Mn_3Ga

H. Kurt,[a] K. Rode, H. Tokuc, P. Stamenov, M. Venkatesan, and J. M. D. Coey
CRANN and School of Physics, Trinity College, Dublin 2, Ireland

(Received 27 July 2012; accepted 12 November 2012; published online 3 December 2012)

Oriented *c*-axis films of the hexagonal triangular antiferromagnetic ε-Mn_3Ga have been used in bottom-pinned synthetic antiferromagnet magnetic tunnel junctions with MgO barriers, which show up to 150% tunneling magnetoresistance at room temperature. Exchange bias fields as high as 150 mT can be achieved for samples field-cooled from 100 °C. Thin films of the antiferromagnet have a Néel temperature in excess of 650 K and provide an interface exchange energy with CoFe of 0.09 mJ m^{-2}. They show an isotropic uncompensated magnetization of $M_s = 48$ kA m^{-1}, with a coercivity $\mu_0 H_c > 3$ T. © *2012 American Institute of Physics*. [http://dx.doi.org/10.1063/1.4768941]

The exchange interaction at the interface between antiferromagnetic (AF) and ferromagnetic (F) core/shell nanoparticles[1] or bilayer thin films[2,3] can shift the hysteresis loop of the ferromagnet laterally when the system is field-cooled through a temperature known as the blocking temperature (T_B) of the antiferromagnet, which should be lower than the Curie temperature (T_C) of the ferromagnet. The blocking temperature, below which the loop shift known as exchange bias can be established, is generally lower than the Néel temperature (T_N) of the antiferromagnet. The shift in the hysteresis loop is thought to be related to frustration of uncompensated spins at the AF/F interface and/or grain boundaries.[4–6] Exchange-bias is used in giant magnetoresistance (GMR) and magnetic tunnel junction (MTJ) spin valve sensors and magnetic random access memories (MRAMs) to pin the magnetization of the ferromagnetic fixed layer. The strength of the exchange bias depends strongly on the magnetic structure, anisotropy, crystalline order, thickness, and texture of the antiferromagnet for a given system.[5,7–10] The origin of the effect is still under discussion, and there are several alternative models to explain this remarkable and useful magnetic phenomenon.[5,6,11]

The first practical application of exchange bias, and indeed the first practical use of an antiferromagnet (NiO), was in GMR read heads for hard disc recording. Several other antiferromagnetic systems including Fe-Mn, Pt-Mn, and Ir-Mn are now used to induce exchange bias in magnetic thin film devices,[11] but the most commonly used material is disordered fcc γ$Mn_{1-x}Ir_x$, for which the T_N ranges from 570 K for x = 0.08 to 730 K for x = 0.25.[12,13] The magnetic structure of the disordered γ phase determined by neutron diffraction shows two possible arrangement of spins; a collinear spin state with moments aligned with an ⟨001⟩ axis, and an alternative where spins on each of four sublattices are aligned with ⟨111⟩ axes.[14] The ordered phase crystallizes in the cubic Cu_3Au structure with a higher $T_N = 960$ K, where the Mn spins are confined in the (111) plane with an angle of 120° between them, forming a triangular antiferromagnet, as determined by neutron diffraction.[13] The source of the anisotropy in $IrMn_3$ is the strong spin-orbit interaction associated with the heavy Ir atoms.

Here, we present oriented films of ε-Mn_3Ga (0001)—a hexagonal triangular antiferromagnet—for use in MTJs with MgO barriers. $Mn_{3-x}Ga$ ($0 \leq x \leq 1$) is a versatile material with two distinct crystalline phases which exhibit different magnetic properties.[15] The tetragonal $D0_{22}$ ε_1-phase is ferrimagnetic with substantial uniaxial anisotropy combined with a high spin polarization[15–21] and a Curie temperature that would be higher than 770 K, if the material did not undergo a structural phase transition to the hexagonal $D0_{19}$ ε-phase. A neutron diffraction study of bulk material of composition $Mn_{2.85}Ga_{1.15}$ indicated that it is a triangular antiferromagnet with $T_N = 470 \pm 10$ K, and a small uncompensated ferromagnetic moment of 0.045 μ_B fu^{-1} that disappears at T_N.[22] The lattice parameters of bulk ε-Mn_3Ga are $a = 0.5404$ nm and $c = 0.4357$ nm. The basic magnetic structure of Mn atoms is inverse triangular, where the chirality of the two spin triangles in the unit cell are opposite; one of the Mn spins points at an angle of 45° from the crystalline ***a*** axis as shown in Fig. 1 and the others are at ±120° intervals.[22] The triangular spin structures found in hexagonal Mn_3X compounds are thought to be stabilized by the Dzyaloshinskii-Moriya interaction $\mathscr{D}_{ij}.[\boldsymbol{S}_i \times \boldsymbol{S}_j]$, where the interaction vector $\mathscr{D}$ lies along the ***c***-axis.[23–25] The weak moment has been attributed to a slight tendency of the moments to align with easy directions in the plane.[24]

Like the tetragonal $D0_{22}$ phase of $Mn_{3-x}Ga$, the hexagonal $D0_{19}$ phase can also crystallize in a range of composition $0 \leq x \leq 1$, with only slight changes in the lattice parameters. We find that oriented c-axis films of hexagonal Mn_3Ga are best grown on Ru (0001), ($2\ a_{Ru} = 0.540$ nm) due to near-perfect lattice matching. The Mn_3Ga is sputtered from a stoichiometric target. The X-ray diffraction pattern of a 60 nm thick Mn_3Ga film grown on a Ta (5)/Ru (30) seed layer shows that it is well-crystallized with a ***c***-axis texture, as shown in Fig. 2. The feature at $2\theta = 37.5°$ is a residual forbidden (002) Si reflection. There is no sign of the $D0_{22}$ phase, which gives X-ray peaks at 25.1° and 51.5°. Further analysis of the structure of the films was conducted on thin sections in a high resolution transmission electron microscope. We carried out microscopy and diffraction studies of a thin section of the Mn_3Ga film deposited on Ru, as in the MTJ device. We confirm the hexagonal lattice structure, and

[a]Present address: Engineering Physics Department, Istanbul Medeniyet University, Göztepe Kadıköy, Istanbul, Turkey. Email: kurth@medeniyet.edu.tr.

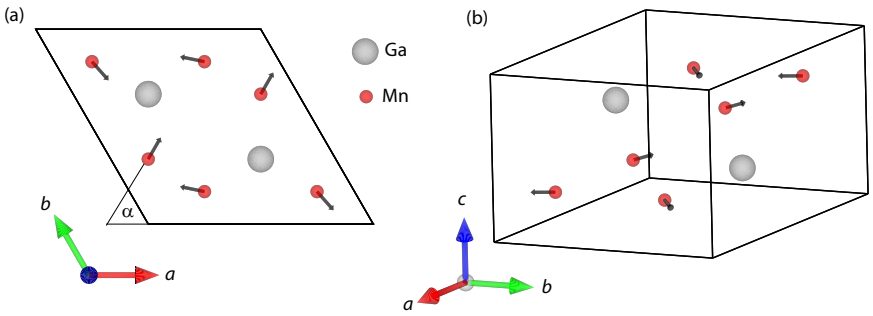

FIG. 1. (a) The basal plane of ε-Mn_3Ga. The arrows represent the directions of magnetic moments on Mn atoms in their ground state. The first Mn moment makes an angle $\alpha = 45°$ with crystalline a axis and the angles between the Mn moments in the same plane are 120° forming a triangular antiferromagnetic structure. (b) 3D view of the unit cell.

find lattice parameters $a = 0.531$ nm and $c = 0.435$ nm, as expected for the $D0_{19}$ unit cell. We also checked the Mn:Ga ratio in the TEM using energy-dispersive X-ray analysis and find a value of 3.0:1, with an error of 10%.

Bottom-pinned MTJs with a synthetic antiferromagnetic (SAF) pinned layer have been grown on thermally oxidized Si wafers by sputtering in our high vacuum Shamrock cluster deposition system. The ε-Mn_3Ga (0001) layer was grown on a lattice-matched Ru (0001) seed layer. Initially, Ta (5)/Ru (30) (all thickness in nm) is deposited at ambient temperature, which produces the ***c***-axis texture on the Ru surface. The wafer is heated to 400 °C and ε-Mn_3Ga (10 or 15 nm) is deposited on the Ru. The wafer is then cooled to room temperature in high vacuum (2×10^{-8} Torr) and the stack $Co_{90}Fe_{10}$ (2.5)/Ru (0.9)/$Co_{40}Fe_{40}B_{20}$ (3)/MgO (2.5)/$Co_{40}Fe_{40}B_{20}$ (3)/Ta (5)/Ru (5) is deposited at ambient temperature. All metallic layers were dc-magnetron sputtered and the MgO was rf-sputtered from a target-facing-target source.[26] The MTJs were patterned into 4×4, 4×12, and 10×10 μm pillars using conventional UV lithography and argon ion milling. The patterned samples are postannealed in high vacuum at $T_a = 100$–350 °C in a 0.8 T magnetic field applied in the plane of the samples both to crystallize the $Co_{40}Fe_{40}B_{20}$ and set the exchange bias. The magnetoresistance measurements were made at room temperature using the four-probe method. MTJs were made with 10 and 15 nm thick ε-Mn_3Ga layers, but the results in both cases were similar. The samples used for magnetization measurements were unpatterned, but annealed at 100 °C, 200 °C, or 300 °C for an hour, with or without the 0.8 T field.

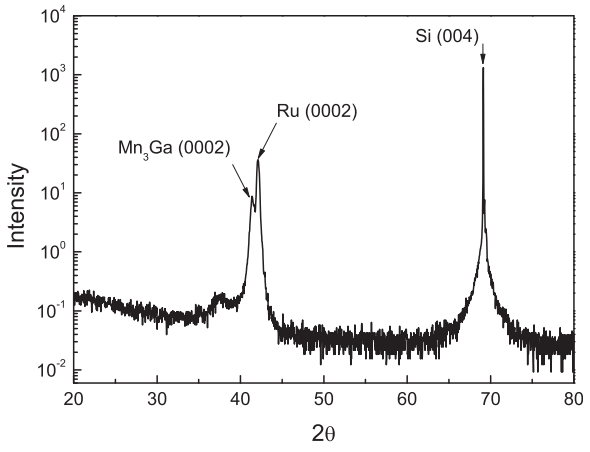

FIG. 2. 2θ X-ray diffraction scan of an oriented ε-Mn_3Ga film grown on a Ru seed layer. The c-parameter for the film is 0.4347 nm.

Large exchange bias fields are observed for all MTJs annealed at 300 °C and below, but the tunneling magnetoresistance (TMR) is low at 100 °C and 200 °C for these junctions due to the partly amorphous nature of the CoFeB electrodes, which are not fully crystallized at these temperatures. High TMR is only achieved when CoFe is crystallized and the boron is expelled.[27,28] The MTJs annealed at higher temperatures have better TMR ratios, but the higher-temperature annealing reduces the exchange bias field H_{eb}, which we define as the value at which the TMR drops to half its maximum value (Figure 3(b)). According to that figure, T_B is about 375 °C, which is considerably higher than the bulk Néel temperature. We conclude that the Néel temperature in these films is at least 180 K greater than it is in the bulk. The high Néel temperature was confirmed by thermal scans of the magnetization, up to 400 K.

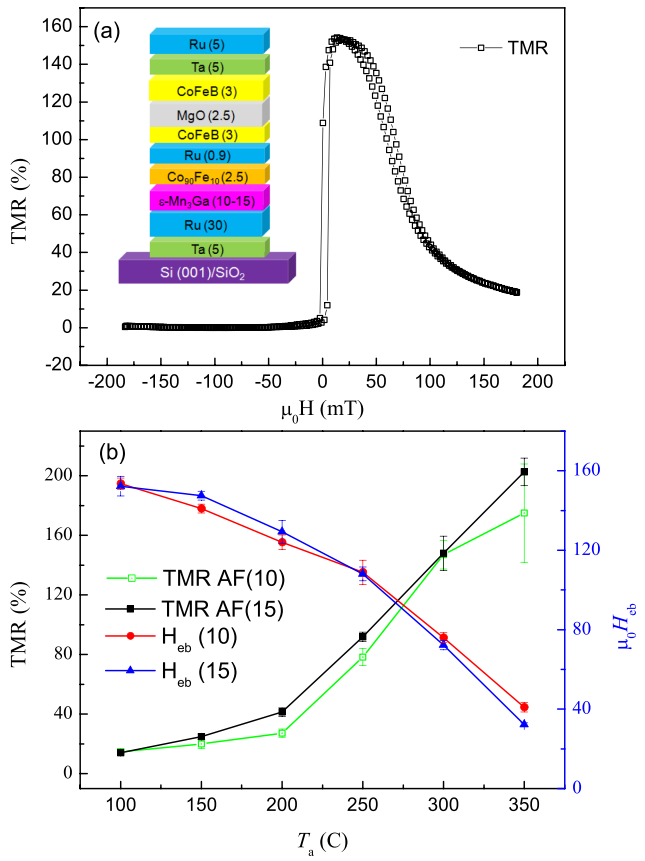

FIG. 3. (a) TMR vs. external field applied along the exchange bias direction of a representative MTJ with 10 nm thick ε-Mn_3Ga antiferromagnet annealed at 300 °C. (b) TMR and exchange bias field H_{ex} of MTJs with 10 and 15 nm thick ε-Mn_3Ga layers at different annealing temperatures. The error bars represent averages of 5–12 samples per point.

A possible contributing factor to the loss of exchange bias at temperatures close to T_B is the degradation of the Mn_3Ga layer due to atomic diffusion. Mn diffusion out of IrMn, becomes significant on annealing at 400 °C, has been shown to decrease exchange bias in MTJs.[29,30] In the case of ε-Mn_3Ga, the degradation of exchange bias becomes significant on annealing above 300 °C, which is not high enough to crystallize CoFeB completely. Nevertheless a 150% TMR at room temperature with $\mu_0 H_{eb} = 75$ mT is achieved, as shown in Fig. 3(a), which is good enough for some applications. Figure 3(b) compares the variation of TMR and exchange bias field at various annealing temperatures for stacks with both 10 and 15 nm thick ε-Mn_3Ga layers. TMR values are approximately the same for both at the best annealing temperature of 300 °C. Interfacial alloying, where Ga atoms from Mn_3Ga can easily alloy with Co and Fe, becomes significant above this temperature.[31]

The magnitude of the exchange-bias energy can be estimated from the spin-flop field H_{sf} of the SAF pinned layer, which is close to the exchange bias field, defined above. The spin flop field[32] is

$$H_{sf} = 2(H_{ex}H_{eb})^{\frac{1}{2}}, \quad (1)$$

where H_{ex} is the exchange field coupling the two ferromagnetic layers of the $Co_{90}Fe_{10}$ (2.5)/Ru (0.9)/$Co_{40}Fe_{40}B_{20}$ (3) SAF which each have magnetic moment m, and H_{eb} is the anisotropy field associated with the exchange bias. First, we must determine H_{ex}. Figure 4 shows the two in-plane magnetization curves of the complete stack annealed at 200 °C in the 0.8 T field. The free layer switches is a small field, but the SAF is gradually aligned when the field is applied in the x-direction perpendicular to the exchange bias direction, reaching saturation for $\mu_0 H_x = 0.5$ T. The in-plane SAF sublattice deflection angle θ is given by $\sin\theta = H_x/H_{ex}$, hence $\mu_0 H_{ex} = 0.5$ T. We see from the figure that $m = 1.0 \times 10^{-7}$ A m^2. The sample has area $A = 6 \times 6$ mm^2, so the exchange energy density for the SAF is $\sigma = m\mu_0 H_{ex}/A = 1.4$ mJ m^{-2}. The spin flop is evident in the third quadrant of the magnetization curve in Fig. 4(b), when the field is applied in the y-direction. The field is $\mu_0 H_{sf} = 250$ mT, hence from Eq. (1) $\mu_0 H_{eb} = 31$ mT, and the corresponding exchange bias energy density is 0.09 mJ m^{-2}. This is about half the value for $IrMn_3$ (0.19 mJ m^{-2}) and 50% greater than NiO (0.06 mJ m^{-2}).[32] The $IrMn_3$ antiferromagnet commonly used in magnetic devices has a disordered fcc structure, whereas the ε-Mn_3Ga has an ordered hexagonal structure.

Finally, we comment on the origin of the weak ferromagnetic moment in our ε-Mn_3Ga films. The hysteresis loops measured for a film with the field applied in-plane or perpendicular to the plane are shown in Fig. 5. The magnetization of 47 kA m^{-1} corresponds to a moment of 0.09 μ_B per Mn, compared to 0.015 μ_B per Mn reported in bulk material. The manganese atomic moment is 2.4 μ_B, so the spins are canted by about 2-3 degrees. Weak moments have also been reported in other $D0_{19}$ Mn compounds,[23–25] where they have been associated with a slight deformation of the Mn spin directions towards the in-plane anisotropy axes. However, the data in Fig. 5 show that the weak moment is practically isotropic with a remanence ratio of ~0.8 in both directions, which suggests that it arises from exchange rather than anisotropy. The Dzyaloshinskii-Moriya interaction is not responsible, because it can only produce an in-plane moment, since $\mathscr{D}$ has to lie along the $\boldsymbol{c}$-axis. A possible origin is ordered vacancies, or excess Ge on the Mn sites, which may also relieve the frustration of the sublattices, increasing the exchange energy density and the magnetic ordering temperature. The loop is not quite saturated in 5 T, as confirmed by measuring the magnetization out to 14 T in a physical property measurement system (PPMS), but the coercivity at

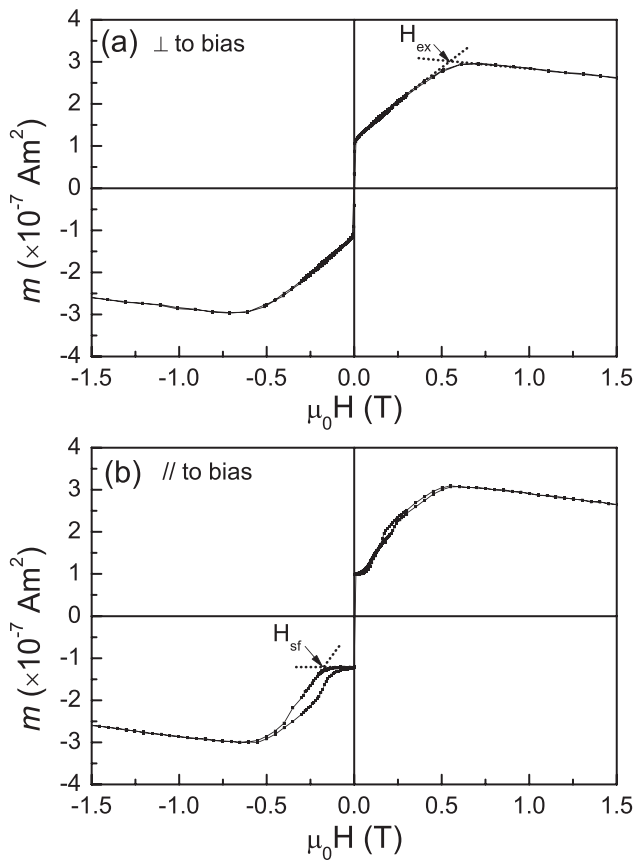

FIG. 4. In-plane magnetization curves of the MTJ stack annealed at 200 °C measured (a) with the field applied perpendicular to the exchange-bias direction and (b) with the field applied along the exchange bias direction. The negative slope above 0.5 T is due to the diamagnetic contribution from the Si substrate.

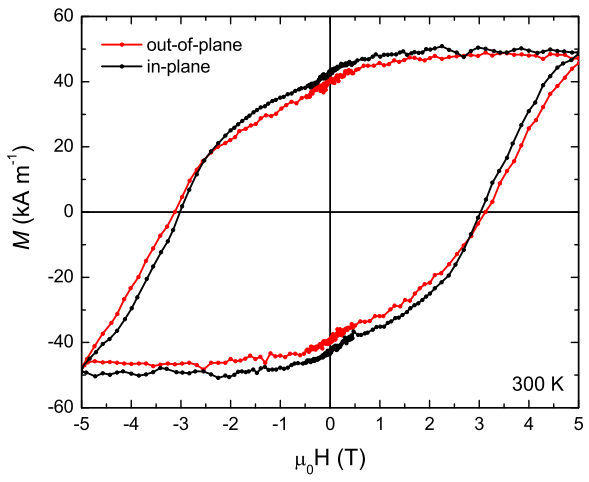

FIG. 5. Room-temperature hysteresis loops for a 60 nm ε-Mn_3Ga film, measured parallel and perpendicular to the film plane in a SQUID magnetometer.

room temperature is slightly in excess of 3 T. A large coercivity often goes hand-in-hand with a small magnetization, since the coercivity is a fraction α of the anisotropy field $2K_u/\mu_0 M_s$, where K_u is the uniaxial anisotropy of whatever origin. For example, if α were 0.3, K_u would be about 300 kJ m^{-3}.

In conclusion, we demonstrated the use of hexagonal Mn_3Ga—a triangular antiferromagnet—in MgO-barrier MTJs. By annealing at low temperature using 10 nm thick ε-Mn_3Ga, exchange bias fields up to 150 mT can be achieved which is a remarkably large value for an antiferromagnet that contains no heavy elements like Ir or Pt. The temperature needed to set the bias is significantly lower than for $IrMn_3$. The large exchange bias is attributed to the frustrated triangular antiferromagnetic structure, which is easily perturbed by exchange coupling to the adjacent ferromagnetic layer. This triangular antiferromagnet could be useful when it is necessary to set exchange anisotropy at a low annealing temperature.

This work was supported by Science Foundation Ireland as part of the NISE project, contract 10/IN1.13006, and conducted under the framework of the INSPIRE programme, funded by the Irish Government's Programme for Research in Third Level Institutions, Cycle 4, National Development Plan 2007-2013. We are grateful to Clive Downing of the CRANN Advanced Microscopy Laboratory for the TEM analysis.

[1]W. H. Meiklejohn and C. P. Bean, Phys. Rev. **102**, 1413 (1956).
[2]L. Néel, Ann. Phys. (Paris) **2**, 61 (1967).
[3]D. Paccard, C. Schlenker, O. Massenet, R. Montmory, and A. Yelon, Phys. Status Solidi B **16**, 301 (1966).
[4]W. H. Meiklejohn, J. Appl. Phys. **33**, 1328 (1962).
[5]J. Nogués and I. K. Schuller, J. Magn. Magn. Mater. **192**, 203 (1999).
[6]A. E. Berkowitz and K. Takano, J. Magn. Magn. Mater. **200**, 552 (1999).
[7]N. P. Aley, R. Kroeger, B. Lafferty, J. Agnew, Y. Lu, and K. O'Grady, IEEE Trans. Magn. **45**, 3869 (2009).
[8]K. Imakita, M. Tsunoda, and M. Takahashi, Appl. Phys. Lett. **85**, 3812 (2004).
[9]C. Mitsumata, A. Sakuma, and K. Fukamichi, IEEE Trans. Magn. **41**, 2700 (2005).
[10]C. Mitsumata, A. Sakuma, and K. Fukamichi, Phys. Rev. B **68**, 014437 (2003).
[11]J. Nogués, J. Sort, V. Langlais, V. Skumryev, S. Suriñach, J. S. Muñoz, and M. D. Baró, Phys. Rep. **422**, 65 (2005).
[12]T. Yamaoka, J. Phys. Soc. Jpn. **36**, 445 (1974).
[13]I. Tomeno, H. N. Fuke, H. Iwasaki, M. Sahashi, and Y. Tsunoda, J. Appl. Phys. **86**, 3853 (1999).
[14]T. Yamaoka, M. Mekata, and H. Takaki, J. Phys. Soc. Jpn. **36**, 438 (1974).
[15]H. Kurt, K. Rode, M. Venkatesan, P. Stamenov, and J. M. D. Coey, Phys. Status Solidi B **248**, 2338 (2011).
[16]H. Kurt, K. Rode, M. Venkatesan, P. Stamenov, and J. M. D. Coey, Phys. Rev. B **83**, 020405 (2011).
[17]F. Wu, E. P. Sajitha, S. Mizukami, D. Watanabe, T. Miyazaki, H. Naganuma, M. Oogane, and Y. Ando, Appl. Phys. Lett. **96**, 042505 (2010).
[18]F. Wu, S. Mizukami, D. Watanabe, H. Naganuma, M. Oogane, Y. Ando, and T. Miyazaki, J. Phys.: Conf. Ser. **200**, 062037 (2010).
[19]F. Wu, S. Mizukami, D. Watanabe, H. Naganuma, M. Oogane, Y. Ando, and T. Miyazaki, Appl. Phys. Lett. **94**, 122503 (2009).
[20]J. Winterlik, B. Balke, G. H. Fecher, C. Felser, M. C. M. Alves, F. Bernardi, and J. Morais, Phys. Rev. B **77**, 054406 (2008).
[21]B. Balke, G. H. Fecher, J. Winterlik, and C. Felser, Appl. Phys. Lett. **90**, 152504 (2007).
[22]E. Krén and G. Kádár, Solid State Commun. **8**, 1653 (1970).
[23]S. Tomiyoshi, S. Abe, Y. Yamaguchi, H. Yamauchi, and H. Yamamoto, J. Magn. Magn. Mater. **54–57** (Part 2), 1001 (1986).
[24]S. Tomiyoshi, Y. Yamaguchi, and T. Nagamiya, J. Magn. Magn. Mater. **31–34**, 629 (1983).
[25]T. Nagamiya, S. Tomiyoshi, and Y. Yamaguchi, Solid State Commun. **42**, 385 (1982).
[26]G. Feng, S. van Dijken, and J. M. D. Coey, Appl. Phys. Lett. **89**, 162501 (2006).
[27]D. D. Djayaprawira, K. Tsunekawa, M. Nagai, H. Maehara, S. Yamagata, N. Watanabe, S. Yuasa, Y. Suzuki, and K. Ando, Appl. Phys. Lett. **86**, 092502 (2005).
[28]H. Kurt, K. Rode, K. Oguz, M. Boese, C. C. Faulkner, and J. M. D. Coey, Appl. Phys. Lett. **96**, 262501 (2010).
[29]D. J. Larson, E. A. Marquis, P. M. Rice, T. J. Prosa, B. P. Geiser, S. H. Yang, and S. S. P. Parkin, Scr. Mater. **64**, 673 (2011).
[30]H. Kurt, K. Oguz, T. Niizeki, and J. M. D. Coey, J. Appl. Phys. **107**, 083920 (2010).
[31]T. B. Massalski, *Binary Alloy Phase Diagrams* (ASM International, 1990).
[32]J. M. D. Coey, *Magnetism and Magnetic Materials* (Cambridge University Press, 2010).